Application of Statistical Parameters in Defining Inlet Airflow Dynamics

LEONARD C. KOSTIN* AND SIDNEY D. MILLSTONE†
North American Rockwell Corporation, Los Angeles, Calif.

During wind-tunnel and flight testing of several inlet duct designs, duct-pressure time histories were recorded on magnetic tape. Preliminary examination of the data indicated the pressure variations to be random processes having Gaussian distribution patterns. Reduction of these data by electronic analog instruments was made to obtain specific statistical parameters; namely, variance, time auto correlations and cross correlations, and power spectral densities. This paper discusses the utilization of these statistical parameters in helping to define the dynamic properties of the inlet duct and the state of the airflow turbulence. Examples are given illustrating the methods and techniques involved.

I. Introduction

THE inclusion of random phenomena as important governing factors in the design of modern aircraft systems introduces an element of uncertainty into the predictions of system responses. Consider the problem of flow instability in inlet ducts and its relation to engine stalls occurring in modern high-speed aircraft. As the inlet system operates more supercritically, boundary-layer flow separation increases, resulting in increased turbulence and spatial distortion at the engine compressor face. The onset of such conditions brings about stall in an apparently random manner; i.e., stall sometimes occurs immediately, sometimes several minutes of operation are possible without stall. If the occurrence of engine stall was a true random phenomenon, then it could not be controlled and, consequently, no further studies, statistical or otherwise, would prove useful. The engineering assumption, of course, is that stall is not a random phenomenon, but a function of nonrandom and controllable effects that can be determined from the flow properties of the inlet-engine system. The basic usefulness of statistical analysis for this study, therefore, lies precisely in its ability to separate the nonrandom effects from what seems to be the more or less random and unpredictable data.

From pressure data taken during both wind-tunnel and flight test of several different inlets, statistical parameters were determined through data-reduction techniques offered by the electronic analog data-reduction instruments. The data were recorded during all stages of inlet operation, including those just prior to stall. The primary purpose of this paper is to discuss the statistical parameters used in evaluating these data and to demonstrate how these parameters can be related to the dynamic state of the inlet-engine system. In describing these parameters, emphasis is placed on their physical interpretations rather than on mathematical descriptions; in fact, because of the complex nature of statistical mathematics, the analytical nature of this work is left entirely to the references listed in the Bibliography. The paper concludes with a brief discussion of the practical aspects of improving over-all performance of an inlet-engine system by specific utilization of the statistical parameters.

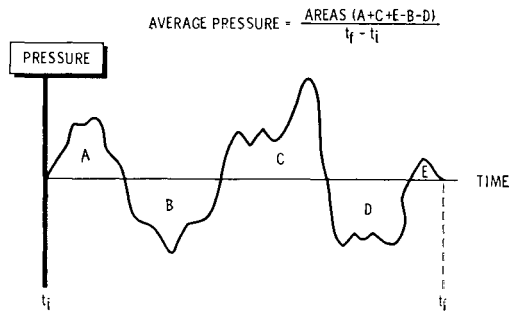

Fig. 1 Average pressure definition.

II. Statistical Parameters and Averages

In this discussion, every statistical parameter is an average or a function of an average; the term "average" being defined in an elementary calculus sense (Fig. 1). The average value of a continuous curve is the net area between the curve and the axis of abscissa divided by the length of this axis between the endpoints of the curve. The basic curves for this application are curves of pressure vs time. The assumption of stationarity requires that an average for the pressure vs time curve computed over any small portion of the curve is the same as the average computed for any other small portion of curve taken at a different time. For example, if a record is 50 sec long as represented by a length of 500 in., then all sections of the curve 10 in. (or 1.0 sec) in length should exhibit the same averages. The average for the pressure vs time curve is called the mean value, and since, for stationary data, this value is constant, only variations about this value will be considered. Therefore, without loss of generality, the

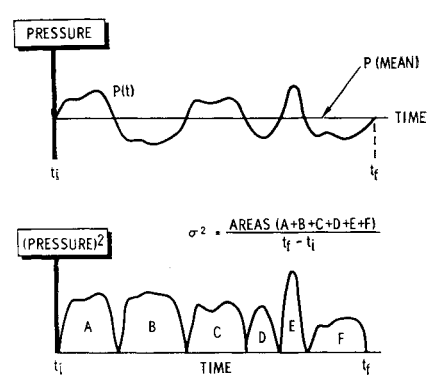

Fig. 2 Mean squared average.

Presented as Paper 68-649 at the AIAA Fourth Joint Propulsion Specialist Conference, Cleveland, Ohio, June 10–14, 1968; submitted June 18, 1968; revision received October 28, 1968.

* Member of the Technical Staff.
† Member of the Technical Staff. Member AIAA.

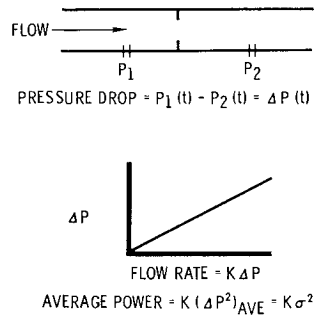

Fig. 3 Power concept for sigma.

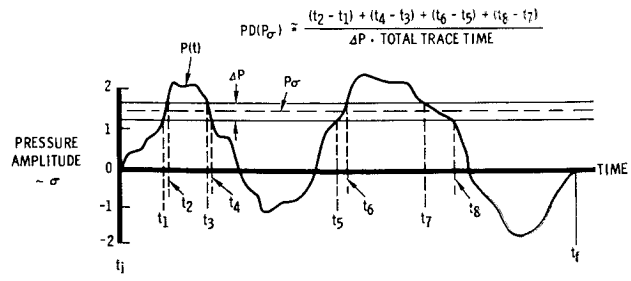

Fig. 5 Calculation of probability density.

mean can be considered zero for the pressure data discussed in this paper.

III. Variance (σ^2) and Standard Deviation (σ)

The variance of a pressure vs time trace (assuming mean zero) is a number representing the average area under the curve of pressure squared vs time (Fig. 2). This parameter, a very important quantity in all branches of statistical analysis, is sometimes known by other names depending on the specific application. In engineering applications involving turbulent pressure data, variance is sometimes called the mean squared pressure value and, not infrequently, is spoken of as the "average power" in a pressure vs time trace. It is important to note that this number does not represent system power in the inlet-engine combination or in the airflow itself. However, variance does represent power in the sense that had the pressure trace been obtained under fairly restrictive conditions (Fig. 3) then the variance would be directly proportional to the power in the airflow system.

The standard deviation (σ, square root of variance) is the primary measure of airflow turbulence amplitude. In engineering applications, this term is generally called the rms (root mean squared) value and, when multiplied by 6, represents, for all practical purposes, the peak-to-peak pressure envelope. The value of σ is perhaps the easiest statistical quantity to obtain from the pressure trace. In practice, the value is read directly from a magnetic tape data record using a random-noise voltmeter that reads true rms volts. By calibration, the instantaneous pressure can be read directly in multiples of sigma.

Standard deviation or variance can be used to compare the relative amounts of energy transmitted down the duct by different pressure functions. For example, two functions having the same σ value will transmit the same amount of energy. However, it is important to note that if one function is purely sinusoidal and the other function is representative of random turbulence, the peak-to-peak maximum amplitude of the turbulent wave will be 6σ, while the peak-to-peak amplitude of the sine wave will only be 2.8σ. From an energy transmission point of view, therefore, turbulent pressures with the same peak-to-peak maximum-amplitude variation as a sine wave pressure disturbance will transmit far less energy. This could prove important, particularly if peak-to-peak value is more important than energy transmission in producing stall.

The variation of σ as a function of inlet total pressure recovery is shown in Fig. 4. These data, recorded during wind-tunnel tests of a mixed compression inlet at Mach 2.2, show increasing turbulence as inlet operation becomes more supercritical, i.e., as total pressure recovery decreases.

IV. Probability Density

The probability density curve, for a pressure vs time trace, indicates the percentage of time that the amplitude of the given trace lies within any arbitrarily specified amplitude range. The curve itself is obtained by considering a small strip of amplitude width ΔP superimposed on the trace at an arbitrary amplitude $P\sigma$ (Fig. 5). By moving the strip through the amplitude range from -3σ to $+3\sigma$, the entire plot can be obtained as a function of the rms amplitude. The probability density at the given point $P\sigma$ is calculated from

$$PD(P\sigma) = (1/\Delta P)(\text{probability trace is within } \Delta P)$$

The probability term in this expression is defined by the percentage of time the trace is actually within the strip and is calculated as shown in Fig. 5.

When sample functions are continuous, the purely random stationary data will exhibit the familiar bell-shaped probability density curve called the normal, or Gaussian, density shown in Fig. 6. The area under specific portions of the curve indicates the percentage of time that the instantaneous amplitude of a pressure wave will be within the specified amplitude range; in other words, the probability that an instantaneous pressure reading will be within the specified

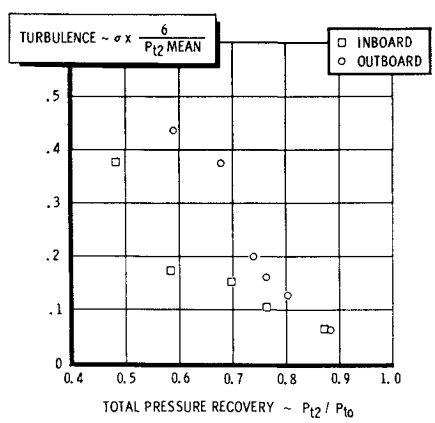

Fig. 4 Turbulence variation with total pressure recovery.

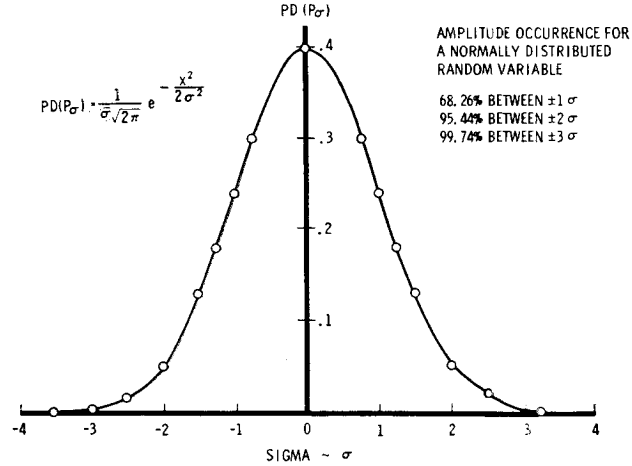

Fig. 6 Normal or Gaussian probability density curve.

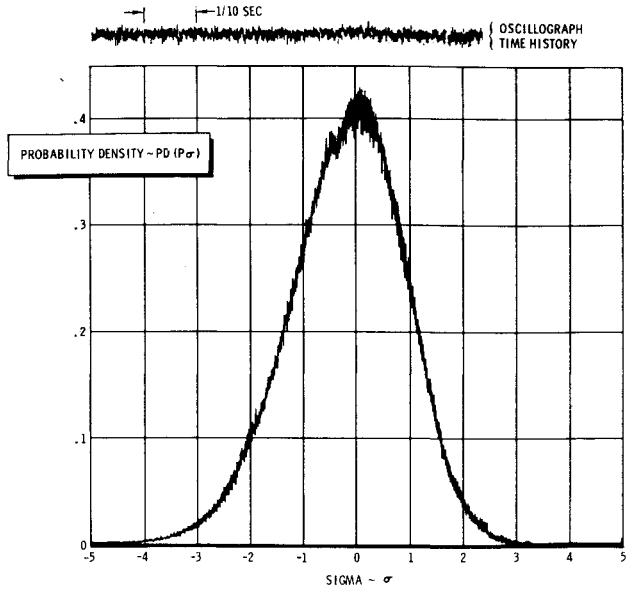

Fig. 7 Probability density histogram for random noise.

region. Thus, we note from the normal density curve of Fig. 6 that the probability of an instantaneous amplitude reading having a value between $\pm 1\sigma$ is 68.3% and that 99.7% of all instantaneous readings will lie between $\pm 3\sigma$.

Deviations of the pressure wave probability density curves from the Gaussian pattern are indications of nonstationary effects taking place during the data recording period. When the curve is approximately normal, but slightly skewed to the left or right of zero deviation, it is an indication that the data are "spikey"; i.e., the data contain very narrow but high-amplitude spikes randomly distributed on only one side of the zero level.

A typical output from the analog probability density analyzer, called a histogram, is shown in Fig. 7 along with a portion of the oscillograph time history. Such data are typical of inlet duct pressures recorded during both normal inlet recovery operation and operation in recovery ranges producing engine stall. The typical Gaussian pattern of the histogram with only slight variations in skewness, testifies to the basically Gaussian character of inlet turbulence in all stages of inlet recovery operation.

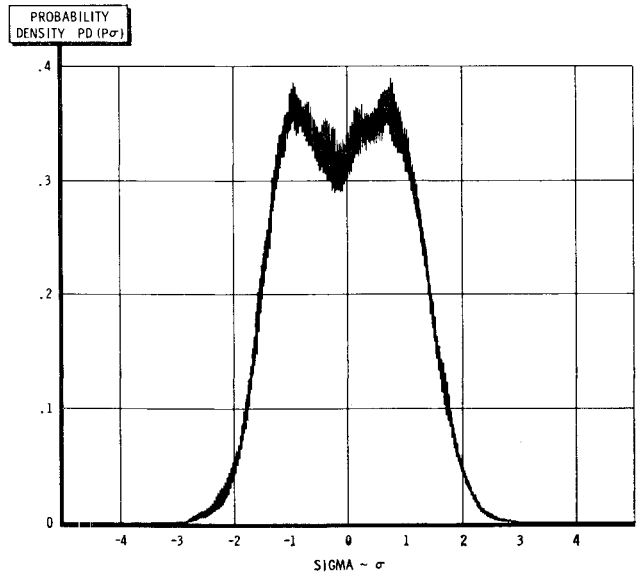

Fig. 8 Probability density histogram for sinusoidal disturbance in random noise.

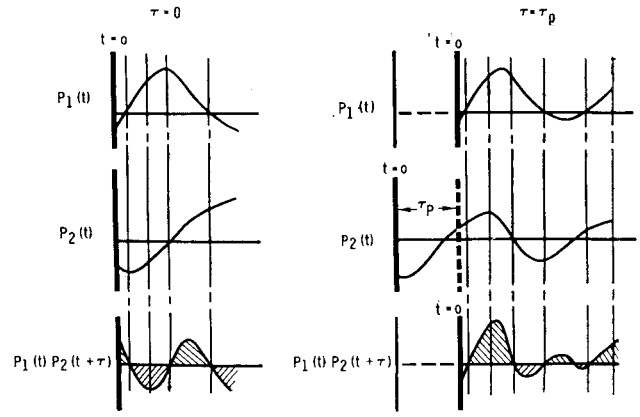

Fig. 9 Delay curve for correlation.

More spectacular nonstationary effects are revealed by a histogram when external nonrandom disturbances are applied to the duct airflow. A probability density plot in which the exit airflow was varied sinusoidally is shown in Fig. 8. The dip in the center is clear evidence of a basically sinusoidal component affecting the turbulence measurements. For such cases, turbulence can be characterized as the sum of two components, namely, a Guassian random noise component and a sinusoidal component.

V. Auto-Correlation and Cross-Correlation

When two pressure traces are superimposed, point-by-point ordinate multiplication of the two traces yields a new curve with ordinate units of pressure squared as a function of time. The point-by-point multiplication is performed for an arbitrary time delay τ in which one trace is purposely delayed in time with respect to the other (Fig. 9). The resulting curve becomes a function of τ, delay being defined as positive (curve a delayed with respect to curve b) or negative (curve b delayed with respect to curve a).

When two pressure traces are identical (i.e., both represent the output of a single pressure transducer), the average area under the pressure-squared curve is a point on the auto-correlation function. This function provides information about airflow at a specific duct location. When two pressure traces represent data taken simultaneously from two separate transducers, the average area under the pressure-squared curve is a point on a cross-correlation function. This function gives information only about the relative conditions of the airflow at two different duct locations.

One point of an auto-correlation function is derived from Fig. 2. Auto-correlation, at $\tau = 0$, represents variance and

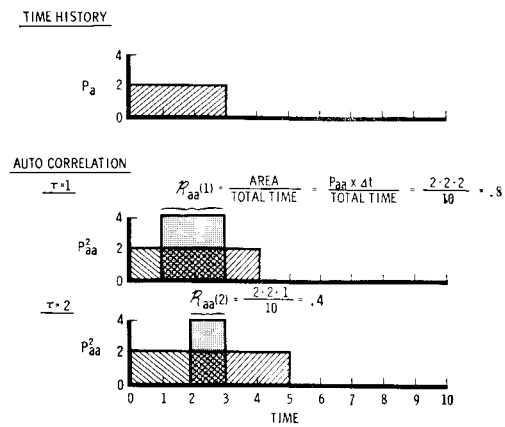

Fig. 10 Auto-correlation for square pulse.

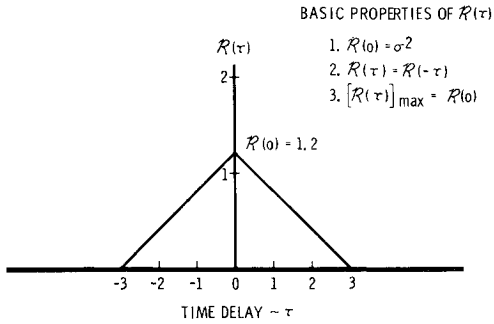

Fig. 11 Correlation points for a square wave.

is normally expressed as

$$\mathcal{R}_{aa}(0) = \sigma^2$$

Examples of auto-correlation calculations for a square pulse at two different values of τ are given in Fig. 10. The over-all auto-correlation function for this case is given in Fig. 11, where the basic properties of all auto-correlation functions are described. Typical auto-correlation functions for pure random pressure data will exhibit a high value at $\tau = 0$ and then drop off rapidly to zero. The function then remains at zero for all subsequent values of τ. When high values of correlation exist for large values of τ, it is an almost certain indication that nonrandom phenomena are present.

Figure 12 represents the analog correlation outputs for an engine-hub total pressure probe at two inlet-duct pressure recovery levels. The data were taken during wind-tunnel tests of a mixed compression inlet operating in a started mode. Curve a, representing the high recovery level, is typical of unperturbed, pure, random turbulence data. The auto-correlation function drops from the maximum to zero in 0.5 msec and remains at zero for all larger values of delay. For the low recovery data, curve b, the auto-correlation function not only shows a slower drop-off rate, but also exhibits a damped periodic pattern with a 0.55-sec period. This corresponds to a frequency of 182 Hz, a value which is very close to the organ pipe frequency of the one-end-open, one-end-closed "organ pipe" extending from the internal normal shock to the simulated engine face. This type of damped oscillation pattern is characteristic of what is sometimes called bandwidth limited noise and, in this case, is clearly related to a resonant vibration occurring in the duct. A further observation of curve b shows that steady-state zero correlation was not reached for the range of τ's analyzed. To obtain low-frequency characteristics (large τ), from a correlator whose low-frequency response is limited, the data can be rerecorded on a continuous tape loop that is speeded up in time. The tape loop may then be played at its original speed through the correlator. For this method to work, however, it is necessary that the original data be of sufficient length to supply the speeded up continuous loop. For example, if 5 sec of recorded data are needed to obtain correlation to 15 msec, then 20 sec of data are required to obtain values up to 60 msec.

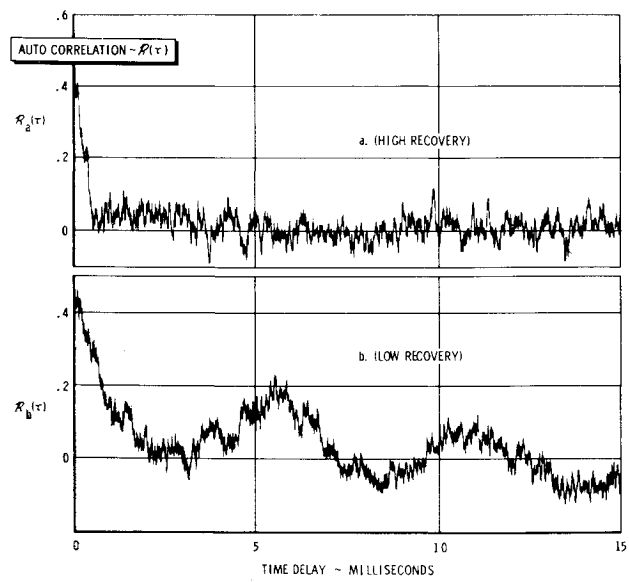

Fig. 12 Auto-correlations for an inlet-duct total pressure probe.

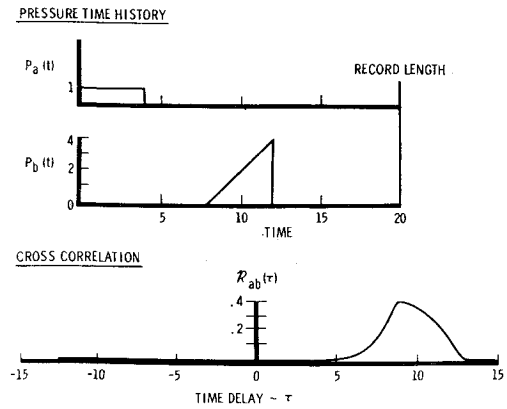

Fig. 13 Cross correlation.

Because the auto-correlation function is symmetrical about the axis $\tau = 0$, there is no need to determine the function for negative values of τ. This is not true for cross-correlation functions as demonstrated by Fig. 13, in which the cross-correlation function exhibits no axial symmetry whatsoever. Consequently, obtaining a cross-correlation for the general case where no symmetries are evident requires both the correlation of curve a delayed with respect to curve b and curve b delayed with respect to curve a. The primary information obtainable from cross-correlation functions is whether or not there is any relationship between pressure disturbances at different inlet-duct locations. If so, what are the time lags or phase angles between the pressures? As such, they are useful for revealing the transport characteristics of known pressure disturbances, indicating the possible sources of nonrandom pressure disturbances in the duct, and for yielding transfer function approximations for the duct properties between two pressure probe locations.

A cross-correlation output from the analog correlator is shown in Fig. 14. The two input pressures are the data from an engine hub total pressure probe and from a duct wall static pressure probe located 13 in. upstream. The inlet

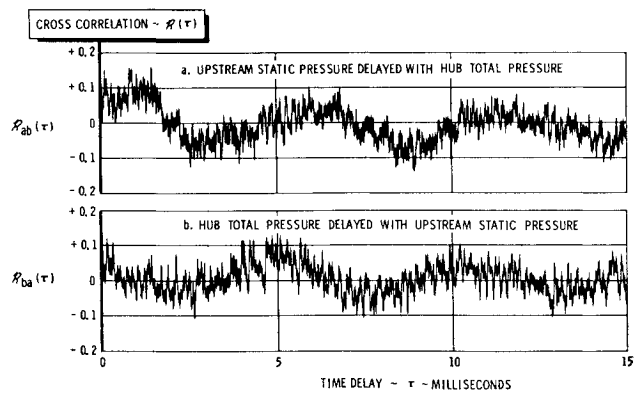

Fig. 14 Cross correlation between two pressures in an inlet duct.

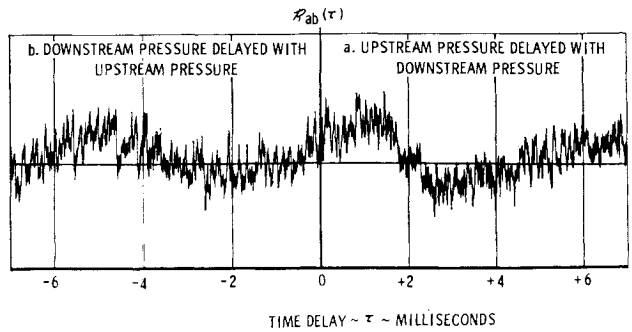

Fig. 15 Over-all cross correlation between two inlet-duct pressures.

operation during this period was at a low (60%) total pressure recovery. To obtain curve a, the static pressure delayed with respect to the total pressure (positive τ), whereas for curve b, the correlator inputs were reversed and the total pressure was delayed with respect to the static (negative τ). By taking the mirror image of b and placing it alongside 14a, the over-all cross-correlation plot on a continuous axis is obtained as shown in Fig. 15.

The outstanding feature of Fig. 15 is the sinusoidal form of the cross correlation. This clearly indicates that some form of periodic pressure variation is being propagated down the duct from the static pressure tap to the total pressure probe at the engine hub. The slight reduction in the amplitudes of successive cycles as τ increases from zero in either direction indicates that the propagation frequency occurs because of a damped resonance effect as opposed to a constant amplitude excitation. The transport time for the propagation can be found by taking the distance from the $\tau = 0$ axis to the nearest positive peak. Because of the poor data at and near $\tau = 0$, the first peak can best be determined by taking the point midway between the two zero crossings on either side of the axis. This gives a propagation transport time of +1.2 msec, indicating the transport direction to be from the static probe towards the total pressure probe.

The transport velocity can be calculated from

$$\text{transport velocity} = \frac{\text{distance between pressure probes}}{\text{transport time}}$$

This transport velocity is made up of two components, namely, the average airflow velocity in the duct and the propagation velocity for sinusoidal waves in still air.

Figure 16 illustrates a cross correlation between two inlet duct static pressures 100 in. apart during a sinusoidal exit area disturbance at 25 Hz. Because of analog data-analysis equipment limitations, to obtain data at this frequency required that the input from the data loop tape be speeded up by a factor of 4. Curve a is the cross correlation for positive τ's in which the upstream static pressure is delayed with respect to the downstream pressure. Curve b is the reversed cross correlation. As might be expected, the correlation plot reveals the periodic oscillations with a period of 40 msec quite clearly. The transport time between the two probes is measured as 9 msec using the same procedure as indicated for Fig. 15. Notice that in this case the transport direction is upstream, against the flow direction, due to the pressure disturbance originating at the downstream end of the duct.

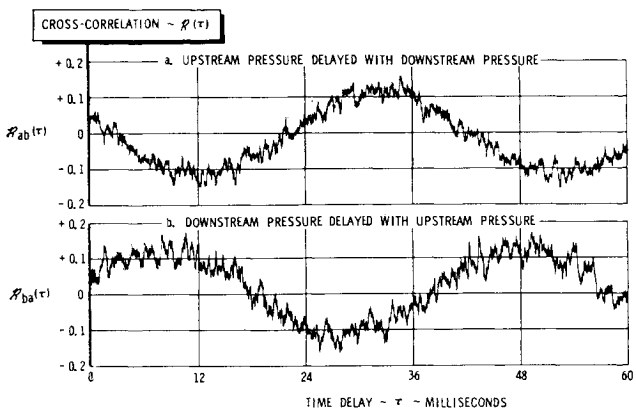

Fig. 16 Cross correlation of inlet-duct pressures during sinusoidal exit area disturbance.

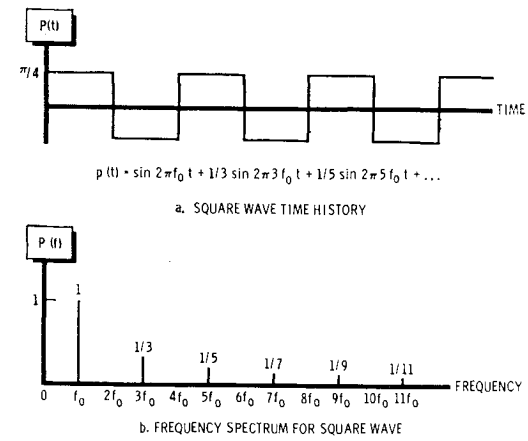

Fig. 17 Fourier representation for square wave.

VI. Power Spectral Density

Power spectral density (PSD) is almost invariably defined as a complex mathematical transform of the auto-correlation function. However, in view of the initial promise to use nothing more complicated than "area under a curve" mathematics, a somewhat different explanation will be presented here. This explanation consists of two basic concepts: 1) The "average power" of a pressure trace is the average area under the pressure-squared curve (σ^2); and 2) an arbitrary pressure vs time trace can be represented, by means of the Fourier analysis, as a linear function (i.e., summation or integration) of sinusoidal components. The first concept already has been discussed (Fig. 2) in the description of variance. The second concept, though somewhat involved analytically, can be explained for purposes of this paper by reference to Figs. 17 and 18.

Figure 17 gives the Fourier representation of the periodic square wave. In Fig. 17a, the pressure is plotted as a function of time, and the Fourier equation for this function is

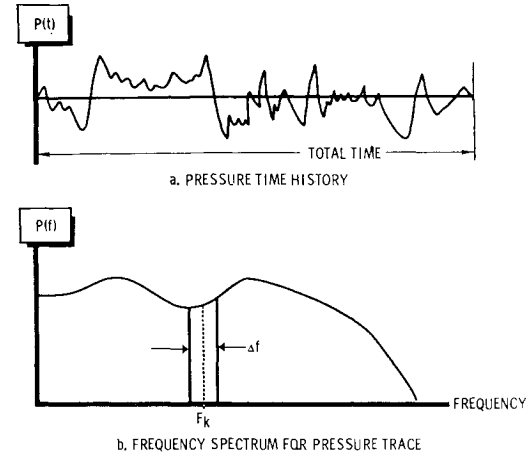

Fig. 18 Fourier representation for nonperiodic trace.

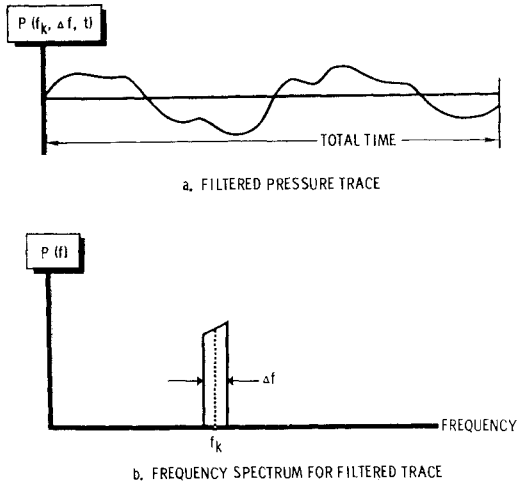

Fig. 19 Fourier representation for filtered trace.

presented explicitly. By plotting the amplitudes of the component frequencies on a frequency axis, the "frequency spectrum" of the square wave is obtained in Fig. 17b. By passing the square wave through a filter that is selective according to frequency, we obtain a new function of time that is no longer a square wave. For example, should the filter drop all frequencies below $4f_0$ and above $8f_0$, the only components of the square wave coming through would be the $5f_0$ and $7f_0$ components. The output wave, which is a new function of time, is therefore

$$P_{\text{out}}(t) = \tfrac{1}{5}\sin 2\pi 5 f_0 t + \tfrac{1}{7}\sin 2\pi 7 f_0 t$$

For the arbitrary pressure wave that is not periodic, the Fourier analysis does not yield the simple summation of discrete frequency components. Instead, we have a continuous spectrum of frequencies which is describable in the form shown by Fig. 18. In this case, passing the pressure function through a filter will then yield a new pressure vs time function that only contains those frequency components within the band of frequencies passed by the filter.

Assume that the pressure wave of Fig. 18 is passed through a narrow-band filter of width Δf about a center frequency point f_k. The result is shown in Fig. 19 as a new pressure vs time trace (curve a), with the frequency spectrum of curve b. In this case, we note carefully that the pressure trace is a function not only of time, but also of the filter bandwidth Δf and the center frequency f_k. Recall now that the average power in the pressure trace of Fig. 18 was given by σ^2 according to the first of our two basic concepts. We can now define the average power in the frequency band Δf at the point f_k by taking the average area under the pressure-squared curve for the pressure trace in Fig. 19:

$$\text{average power at } f_k = \frac{\text{area under } P^2(f_k, \Delta f, t)}{\text{total time}}$$

The power spectral density at f_k is approximated by

$$\text{PSD}(f_k) = (1/\Delta f)(\text{average power at } f_k)$$

By moving the center frequency point throughout the frequency spectrum, the power density then can be determined. It is plotted as a function of frequency for the original pressure vs time curve of Fig. 18.

Power spectral density plots from the spectral density analyzer are illustrated in Figs. 20 and 21. The curves in Fig. 20 represent the same data used for the auto-correlation plots of Fig. 12, i.e., data from an engine-hub total pressure probe at two duct pressure recovery levels. They demonstrate the distribution of energy in the frequency spectrum

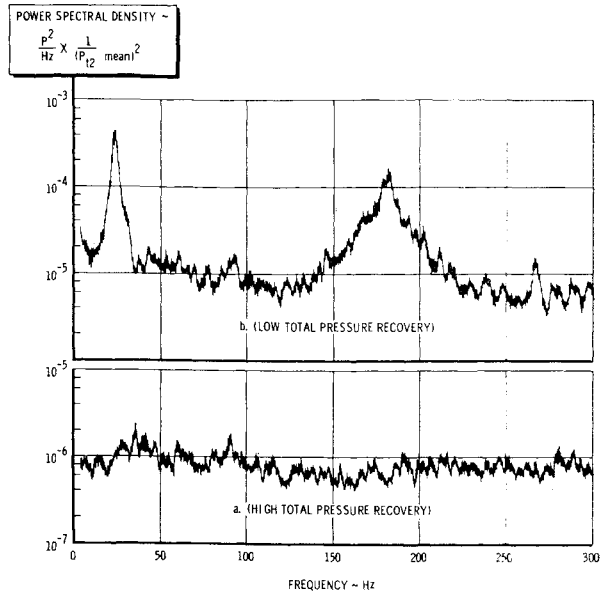

Fig. 20 Power spectral density of an inlet-duct total pressure probe.

of the pressure trace. The PSD values in curve a, high total pressure recovery (90%), are essentially constant over the entire range of frequencies shown. The PSD values in curve b, for an abnormally low-pressure recovery (60%), reveal not only a higher level of energy at all frequencies, but particularly high peaks occurring at 182 and 24 Hz. The peaks represent resonant effects. The 182-Hz peak corresponds to the organ pipe frequency already discussed for Fig. 12. The 24-Hz peak verifies the predictions that low-frequency phenomena occur which are not revealed by Fig. 12. This 24-Hz peak is related to the resonant frequency of a fundamental Helmholtz resonator in which the volume of air in the metering duct section acts as a spring on the air mass in the inlet from the internal normal shock to the simulated engine face.

The sharpness of the amplitude change and the narrowness of the frequency bandwidth for the sinusoidal data, at 25 Hz, are clearly distinguished from the somewhat broader bandwidth and amplitude variation of the resonant peaks. A 70:1 amplitude ratio relative to the nearby frequencies was obtained with sinusoidal data. This is in contrast to the amplitude ratio of the resonant peaks at low recovery levels which varied between 25 and 30.

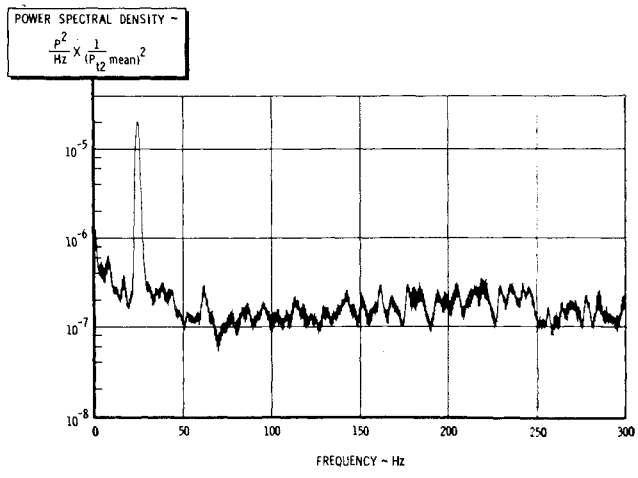

Fig. 21 Power spectral density of an inlet-duct pressure during sinusoidal exit disturbance.

VII. Conclusions

The indications of the data taken and presented so far strongly favor two conclusions:

1) Statistical parameters are measurable quantities for inlet-duct pressures, in the sense that they can be determined and monitored by instrumentation that is presently available.

2) The values obtained for statistical parameters are indicative of the behavior or operational state of the inlet duct. Consequently, they can be used for measurements of changes in the airflow patterns and characteristics that affect both inlet and engine.

These conclusions remove statistical considerations from the realm of mathematical exercises for the statistician and place them in the area of practical design considerations for use by engineers.

Such considerations are already in everyday use for other aerospace vehicle system designs. For example, missile guidance and radar systems have controls that are governed by computers calculating statistical parameters and sending control signals in accordance with the calculations. It is likely that similar applications will be required for inlet-engine control systems. However, before such sophisticated techniques can be useful in inlet applicatons, a great deal has yet to be learned about defining the operational "state" of an inlet-engine system in terms of its statistical parameters. For this purpose, both analog and digital data reduction techniques will be necessary in future tests of controllable inlet-engine systems.

In today's aircraft propulsion system designs, performance values are degraded by the dictates of engine stall and flow-stability margins. The magnitudes of these margins are set by standardized procedures governed by the maximum anticipated extremes of flow. The authors of this paper feel that statistical parameter studies will lead to a substantial reduction in stall margins through better definition of the state of the inlet-engine system at any instant. Performance improvements may come about as the result of control signals sent by on-line computers processing the monitored statistical parameters. Airflow changes could be monitored continuously, permitting inlet operation closer to the critical points of instability.

Bibliography

[1] Bellman, R., *Adaptive Control Processes: A Guided Tour*, Princeton University Press, Princeton, N. J., 1961.

[2] Bendat, J. S. and Piersol, A. G., "Design Considerations and Use of Power Spectral Density Analyzers," Measurement Analysis Corp.; report printed and distributed by Honeywell, Denver, Colo.

[3] Cramer, H. and Leadbetter, M. R., *Stationary and Related Stochastic Processes. Sample Function Properties and Their Applications*, Wiley, New York, 1967.

[4] Gnedenko, *Theory of Probability*, Chelsea Publishing Co., New York, 1962.

[5] Parzen, E., *Modern Probability Theory and Its Applications*, Wiley, New York, 1960.

[6] Thrall, G. P., "An Analysis of Amplitude Probability Measurements," FDL-TDR-64-116, Air Force Flight Dynamics Lab., Air Force Systems Command, Wright-Patterson Air Force Base, Ohio.